# Performance analysis of OFDM modulation on in-vehicle channels in the frequency band up to 100 MHz

Juan José Sánchez-Martínez[1], Ana Belén Vallejo-Mora, José Antonio Cortés,
Francisco Javier Cañete, and Luis Díez
Departamento de Ingeniería de Comunicaciones
E.T.S.I. de Telecomunicación, University of Málaga, Spain
Email: [1]jjsm@ic.uma.es

***Abstract*—This paper analyses the performance of an Orthogonal Frequency Division Multiplexing (OFDM) system on in-vehicle power line channels. The achievable bit-rate as function of the cyclic prefix length and the number of subcarriers is obtained over a set of measured channels. Statistical results are drawn and the system parameters design is undertaken determining the values that maximize the system performance.**

## I. Introduction

In the last years there has been a growing interest in the field of power line communications (PLC) as a high-speed transmission medium. Two main applications for PLC systems have been considered: to integrate them into wide area telecommunications networks as the 'last mile', and to serve as Local Area Networks (LAN's) inside buildings (small offices and homes). Nowadays, a new application is attracting the attention of researchers: the use of in-vehicle power lines for data communication.

Currently, in an automobile there are a great number of sensors and actuators incorporated into systems with different functions (passive and active safety, injection and lighting systems, etc.), which are communicated between them and with a central control system. Up to now, this communication has been carried out through dedicated buses as CAN (Controller Area Network), LIN (Local Interconnect Network) and FlexRay. However, all electronic devices in the car are powered by battery and thus, there is a network (DC lines) which connects them and that brings an alternative solution for communication, using the power lines to transmit both information and the necessary energy. Such alternative offers many advantages: allows reducing the existing wiring dedicated exclusively to data transmission and, therefore, the production cost, also reduces the vehicle weight and the fuel consumption. Moreover, PLC would allow incorporating new functions without the need for additional wiring.

The DC network has a great similarity with the in-home power grid. The characteristics of the links established between elements depend on the lengths of the paths and on the number and type of loads plugged in. A tree-like structure can be inferred and, as consequence of multipath propagation phenomena, channel responses with deep notches are expected. This occurs because the diversity of connected loads causes a signal to suffer multiple reflections in every branch encountered along the path from transmitter to receiver. Multicarrier Modulation (MC) has been proven to be an appropriated technique to cope with the frequency selectivity of channels adjusting the bit-rate per subcarrier. Some papers have already evaluated the adequacy of this technique on vehicles [1], [2], [3], [4], [5], but in this paper we deal with the optimization problem. We determine the system parameters -number of subcarriers and cyclic prefix length- that maximize the system performance and analyze the influence of the engine state on the achievable bit-rate. For this purpose, we have used channel response measurements carried out on a vehicle for three engine states: off, idle and at 2000 rpm [4].

The organization of the paper is as follows. Firstly, both system model and channel model are described in sections II and III respectively. Parameters design and performance of an OFDM system are assessed in section IV. Finally, conclusions are summarized in section V.

## II. System model

An OFDM system with N subcarriers and a cyclic prefix of length *cp* samples is considered. The low pass equivalent of a conventional OFDM system is shown in Fig. 1. The

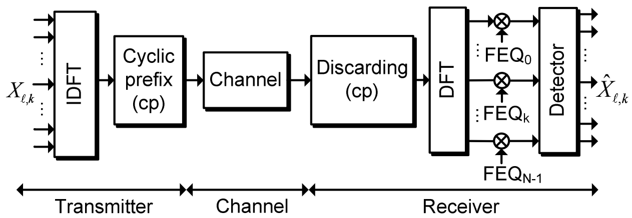


Fig. 1. Functional model of a conventional OFDM system.

inverse Discrete Fourier Transform (IDFT) block acts as the modulator, converting the input streams of N parallel complex numbers $X_{\ell,k}$, into the output stream of N series complex time-domain samples. In this point the orthogonality among subcarriers is guaranteed, which can be maintained even when the signal traverses a time-dispersive channel introducing a guard interval of $cp$ samples, leading to

$$x_\ell(n) = \sum_{k=0}^{N-1} X_{\ell,k} e^{j\frac{2\pi k}{N}(n-cp)}, \quad n = 0..L-1. \tag{1}$$

$X_{\ell,k}$ represents the complex values to be transmitted on each subcarrier, where $k$=0,1...N-1 is the subcarrier index, $\ell$ is the sequential number of the OFDM symbols and L=N+cp. Therefore, the discrete time transmitted signal can be expressed in the form

$$x(n) = \sum_{\ell=-\infty}^{\infty} x_\ell(n-\ell L) w_L(n-\ell L), \tag{2}$$

where $w_L$ is a rectangular window defined as

$$w_L(\mathrm{n}) = \begin{cases} 1 & \text{for} \quad n = 0...L-1 \\ 0 & \qquad\quad \text{otherwise} \end{cases}. \tag{3}$$

The cyclic prefix is removed for each OFDM symbol before entering to the DFT block at the receiver. The values transmitted in each subcarrier can be extracted by performing a N-point DFT over the rectangular windowed input sequence. The equalization process of the received signal is accomplished by means of a frequency equalizer (FEQ) at the outputs of the DFT block in order to compensate for the channel attenuation. The selected FEQ presents the form $FEQ_k = 1/H_k$, where $H_k$ is the value of the channel frequency response at the frequency of the $k$ subcarrier. The adopted FEQ, known as zero-forcing criterion, is the simplest form when there is neither inter-symbol interference (ISI) nor inter-carrier interference (ICI) in the OFDM symbols, what is achieved if the cyclic prefix is larger than the channel impulsive response length.

## III. Channel model

The channel model used in this paper is composed of a linear and time-invariant (LTI) filter and a stationary Gaussian colored noise. The frequency responses of the LTI filter and the noise PSDs are taken from measurements carried out for three engine states: off, idle and at 2000 rpm. Table I summarizes the total number of channels used through the simulations as function of the engine speed. A description of the channel responses and the selected noise PSDs is given in subsections III-A and III-B.

TABLE I
Number of channels used.

| Engine state | Off | Idle | 2000 rpm |
|---|---|---|---|
| Number of channel responses | 12 | 12 | 12 |
| Number of noise PSD | 2 | 2 | 2 |
| Total number of channels | 24 | 24 | 24 |

### A. Channel frequency response

Channel measurements have been carried out in a Fiat automobile. $S_{11}$ and $S_{21}$ parameters have been measured using a Vectorial Network Analyzer (VNA) with $Z_0 = 50\ \Omega$ as reference impedance, being the number of measured discrete frequencies 1601 in the range from 300 kHz to 100 MHz.

TABLE II
Measured Channels

| Transmitter | Receiver |
|---|---|
| BAT | CIG |
| CIG | BAT |
| FrontRTS | RADP |
| RADP | FrontRTS |
| RearRBAC | FUSB |
| RearLPA | FUSA |
| FrontLBE | RADL |
| BAT | RearRBAC |
| RADP | CIG |
| RearLPA | RearRBAC |
| FrontRTS | FrontLBE |
| FUSB | BAT |

The channel frequency responses are computed as

$$H(f) = \frac{S_{21}(f)}{1 + S_{11}(f)}. \tag{4}$$

Twelve different channels have been measured by connecting the selected points in Table II. A link is named as direct if the shortest path between transmitter and receiver does not pass through the battery and as indirect in other case [6]. The link RADP-CIG is the only measured direct channel. Ten access points distributed along the car have been selected, which are utilized as transmitter and receiver nodes. Some points are directly connected to the battery (always powered) and other ones are only powered when the engine is running. The used nomenclature refers to the following systems: the battery (BAT), the cigarette lighter (CIG), the power supply connector (RADP) and the lighting power connector (RADL) of the radio system, the right front turn signal light (FrontRTS), the left low beam headlight (FrontLBE), the left rear parking light (RearLPA), the right back-up light (RearRBAC) and two fuses, one (FUSA) protects circuits as the instrument panel lights, the right rear and left front parking lights and the left license plate light, and the other one (FUSB) protects the front panel power supply, the windscreen wiper motor, the back-up lights and the fuel injection control system.

Fig. 2 represents the 10th and 90th percentiles of the channel frequency response amplitude at each frequency for the three evaluated engine states, computed as

$$|Hx(f)| = CDF^{-1}(f, x\%), \tag{5}$$

with $x = 10$ and $x = 90$, and where $CDF^{-1}(f, x\%)$ is the inverse of the CDF of the channel frequency response amplitude at frequency $f$, $CDF(|H|, f)$. Results exhibit a great frequency variation and in some frequencies there are variations of up to 15 dB for the same percentile among the three engine states. As can be observed, the frequency bands [0-20] MHz and [55-70] MHz exhibit the greatest values.

### B. Noise

Noise signals have been captured on different access points for the three engine states considered. The noise Power Spec-

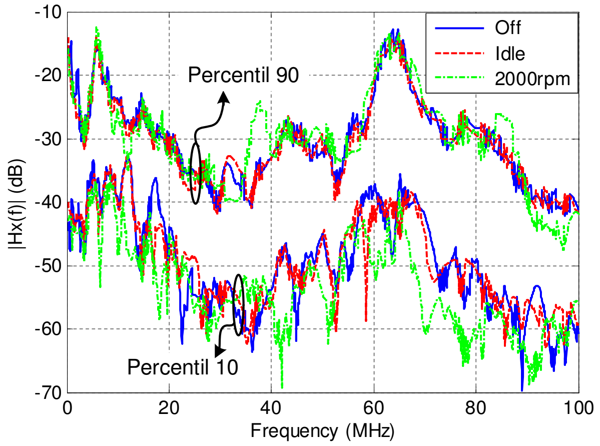


Fig. 2. 10th and 90th percentiles of the channel frequency response amplitude at each frequency.

tral Density (PSD) has been computed by means of averaged periodogram method with a frequency resolution of 10 kHz in the band [0-100] MHz. The two noise PSDs selected as representative of the whole set and that will be used through this paper are plotted in Fig. 3. The background noise floor is between -115 dBm/kHz and -120 dBm/kHz.

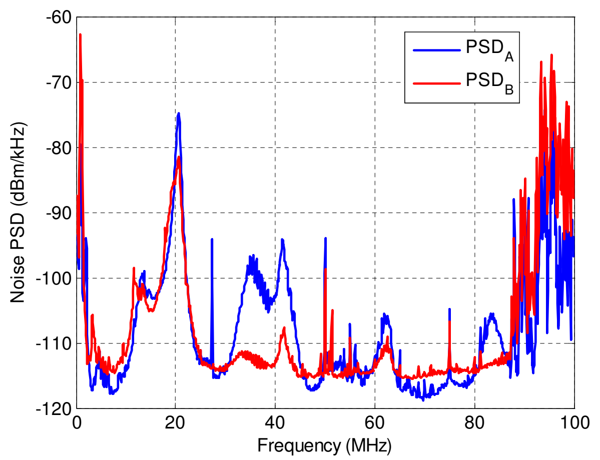


Fig. 3. Estimated noise PSD at two different access points, $PSD_A$ at the battery and $PSD_B$ at the cigarette lighter.

## IV. System Parameters Design

In this section, parameters that maximize the performance of an OFDM system over the measured channels is assessed. Simulations using Binary PSK (BPSK) and square QAM constellations with a maximum of 12 bits per symbol (bit cap used currently in commercial systems) under a BER constraint of $10^{-3}$ are carried out. A transmit signal PSD of -50 dBm/kHz is used, which is compliant with the CISPR 25 standard [7]. Useful expressions to evaluate the bit-rate as function of the cyclic prefix length, *cp*, and the number of subcarriers, *N*, are firstly derived. These expressions will be used after to determine performance according to the achievable bit-rate.

An OFDM system can be seen as a set of $k$ parallel subchannels, where both noise and distortion caused by the channel can be approximated as Gaussian signals. In such conditions the bits per subchannel can be obtained as

$$b_m(k) = \left\lfloor \log_2\left(1 + \frac{SNDR_m(k)}{\Gamma}\right)\right\rfloor, \tag{6}$$

where subindex $m$ refers to the channel number, $SNDR_m$ is the signal to noise plus distortion ratio, $\Gamma$ is a factor which models the capacity loss by using a discrete constellation [8] and $\lfloor x \rfloor$ denotes the integer part of $x$.

Therefore, the achieved bit-rate in the *m-th* channel is determined using the following equation

$$R_m(N, cp) = \frac{f_s}{N + cp}\sum_{k=0}^{N-1} b_m(k), \tag{7}$$

where $f_s$ is the sampling frequency (100 MHz in our case).

### A. Parameterization approach

As seen in (7), achievable bit-rate depends on both values $N$ and $cp$, and consequently there is a trade-off between both parameters that optimizes the system performance. Once $N$ is fixed, there is a particular $cp$ value for each channel that maximize the bit-rate. This value will be the one that is large enough to absorb the channel distortion but considering that the longer the cyclic prefix, the larger the symbol rate loss. Increasing the $cp$ length helps to improve the signal to distortion ratio but at the expense of reducing the signal to noise ratio (the overhead part not used in the detection process increases) and increasing the symbol rate loss. Accordingly, $cp$ is conditioned by the channel under analysis, its delay spread or equivalently the impulsive response effective length, and the noise power. In bad scenarios, with low signal to noise ratios (SNR), optimum $cp$ values will be shorter than in good scenarios with high SNR, but noise is the predominant term.

The bit-rate loss produced in the *m-th* channel by the use of a non-optimum cyclic prefix is given by

$$L_m(N, cp) = 1 - \frac{R_m(N, cp)}{\max\limits_{cp}\{R_m(N, cp)\}}, \tag{8}$$

and the averaged bit-rate loss over the M considered channels is calculated as

$$\overline{L}(N, cp) = \frac{1}{M}\sum_{m=1}^{M} L_m(N, cp). \tag{9}$$

The objective is to minimize the averaged bit-rate loss in (9). A different criterion, and possibly more intuitive, would be to maximize the aggregate bit-rate of all channels, but in such a case, it is possible to obtain as optimum parameters the ones associated with the best channel (the highest SNDR). This would originate a situation where a channel would have a high bit-rate but reducing the transmission capacity in the rest of channels. Hence, the criterion adopted in this paper seems to be a more fair condition, expressed as

$$cp_{opt}(N) = arg \min_{cp}\left\{\overline{L}(N, cp)\right\}. \tag{10}$$

*B. System parameterization*

Fig. 4 shows the logarithm averaged bit-rate loss as a function of the number of subcarriers and the cyclic prefix length for the off state. The shape of the graphic is similar for the other two states, idle and 2000 rpm. This figure addresses that increasing the number of subcarriers always improves the performance because it reduces the distortion due to the channel frequency selectivity and improves the transmission efficiency. Further, it implies a larger window and, from the receiver point of view, it has two positive effects because of the spectrum of the window. It implies a greater spectral containment, and as consequence it helps to reduce the inter-carrier interference and the power noise per subcarrier. The reason is that although the level of the side-lobe of the window is always 13.3 dB under the maximum, the trend of decay is directly related with the window length. The last feature is of relevant interest in colored noise environments like automotive networks.

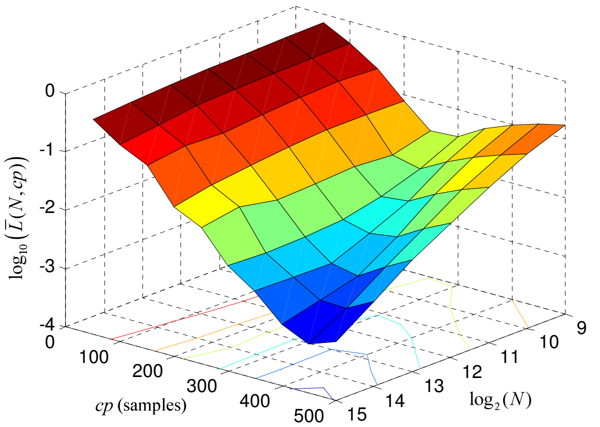


Fig. 4. Averaged bit-rate loss as a function of the number of carriers and the cyclic prefix length.

Table III shows the *cp* values that maximize the system performance for a certain N ($N = 2^c$, with c=9...15), and for the three engine states. As expected, as the number of subcarriers increases the optimum *cp* length increases and the minimum of the averaged bit-rate loss decreases. However, although increasing the number of subcarriers means improving the performance, it supposes a nonlinear computational complexity increase. Defining the aggregate bit-rate for all channels as

$$R(N) = \sum_{m=1}^{M} R_m \left(N, cp_{opt}(N)\right), \qquad (11)$$

we can calculate the aggregate bit rate gain by increasing the number of subcarriers respect to the minimum value $2^9$ (512) as

$$RG(\%) = \left(\frac{R(N)}{R(2^9)} - 1\right) \cdot 100. \qquad (12)$$

Fig. 5 shows the results of evaluating (12). As seen, the aggregate bit-rate gain exhibits a nonlinear dependence on the number of subcarriers. It can be also noticed that gains are higher when the engine is running than when it is turned off. The reason is that the coherence bandwith of the channels in the latter scenario is generally smaller than in the former one. The gain reductions become faster above $2^{12}$ subcarriers. This result, along with the fact that 4096 and 6144 have been set as maximum FFT sizes in the new upcoming standards for in-home PLC, have made us to restrict the number of subcarriers considered in this study to 512, 1024, 2048 and 4096 (all FFT-size are power of two, which facilities hardware implementation).

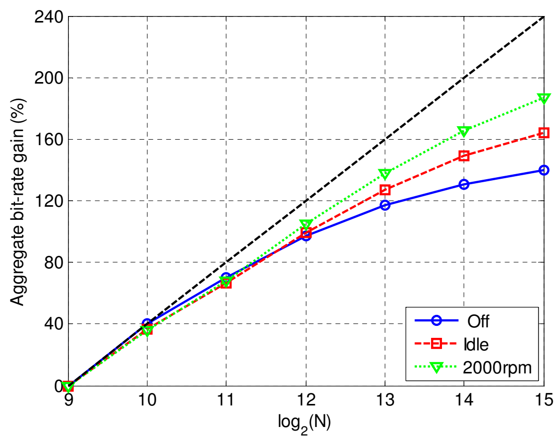


Fig. 5. Aggregate bit-rate gain as a percentage respect to the achieved one with 512 subcarriers for the three engine states.

The logarithm of the averaged bit-rate loss for the off, idle and 2000 rpm engine states is shown in Fig. 6, where the logarithm function has been used for the sake of legibility. For small values of the cyclic prefix, the averaged bit-rate loss diminishes as the cyclic prefix length increases, but once the reduction of the distortion does not compensate for the symbol rate loss, increasing the cyclic prefix length is counterproductive and cause the averaged bit-rate loss to increase too. We can appreciate that the lowest losses are always achieved for the off state and that optimum cyclic prefix lengths are very similar in the three engine states for each number of subcarriers. Further, the low value of the minimum averaged bit-rate losses allows deducing that the dispersion of the optimum values for all channels is small.

Even using the optimum cyclic prefix lengths given in Table III, each channel suffers a certain bit-rate loss because such values are optimum on average. Therefore, it is interesting to compute the distribution of the optimum values per channel, which is an indicative of the channel uniformity. The CDF of the values that maximize the aggregate bit-rate per channel for 1024 and 4096 subcarriers are drawn in Fig. 7 (curves for 512 and 2048 subcarriers exhibit the same tendency). There are differences between the curves for the three engine states, and as expected, the cyclic prefix lengths are longer for 4096 than 1024. The minimum lengths are associated with the direct

TABLE III
OPTIMUM CYCLIC PREFIX LENGTHS ($\mu s$) AS FUNCTION OF THE NUMBER OF CARRIERS

| | Number of subcarriers | | | | | | | | | | | | | |
|---|---|---|---|---|---|---|---|---|---|---|---|---|---|---|
| | $2^9$ | | $2^{10}$ | | $2^{11}$ | | $2^{12}$ | | $2^{13}$ | | $2^{14}$ | | $2^{15}$ | |
| | $cp_{opt}$ | $\overline{L}^{*1}$ | $cp_{opt}$ | $\overline{L}^{*1}$ | $cp_{opt}$ | $\overline{L}^{*1}$ | $cp_{opt}$ | $\overline{L}^{*1}$ | $cp_{opt}$ | $\overline{L}^{*1}$ | $cp_{opt}$ | $\overline{L}^{*1}$ | $cp_{opt}$ | $\overline{L}^{*1}$ |
| Off | 253 | -1.60 | 276 | -1.90 | 315 | -2.15 | 327 | -2.43 | 382 | -2.71 | 420 | -2.89 | 446 | -3.24 |
| Idle | 233 | -1.50 | 255 | -1.89 | 275 | -2.01 | 312 | -2.38 | 372 | -2.52 | 441 | -2.69 | 570 | -2.89 |
| 2000 rpm | 229 | -1.51 | 235 | -1.79 | 275 | -1.93 | 327 | -2.19 | 380 | -2.21 | 502 | -2.46 | 570 | -2.86 |

[1] $\overline{L}^* = \log_{10} \overline{L}$

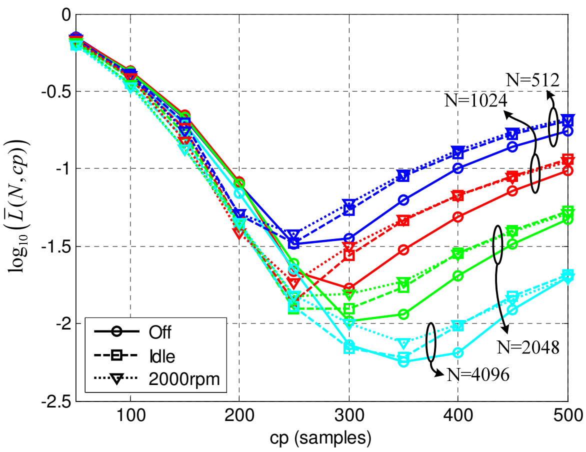


Fig. 6. Averaged bit-rate loss as a function of the number of carriers and the cyclic prefix length.

links, which are characterized by a lower channel dispersion.

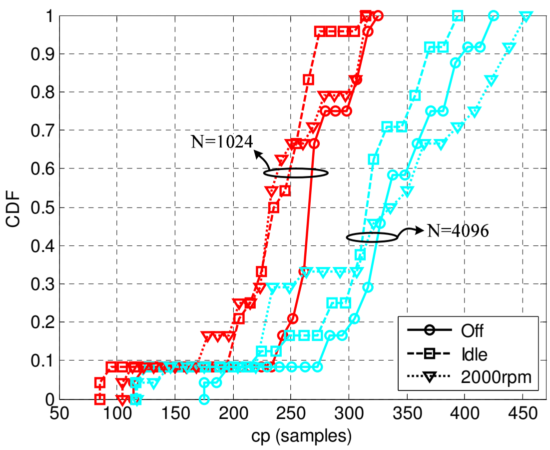


Fig. 7. CDF of the optimum cyclic prefix for each channel for the three engine states and 1024 and 4096 subcarriers.

Regarding values in Table III, it seems that there is no direct relation between the optimum cyclic prefix length and the engine state. However, in all cases, the smallest averaged bit-rate losses are obtained in the off state and the largest in the 2000 rpm state. Subsequent results have been obtained with the values in Table III. Fig. 8 represents the CDF of

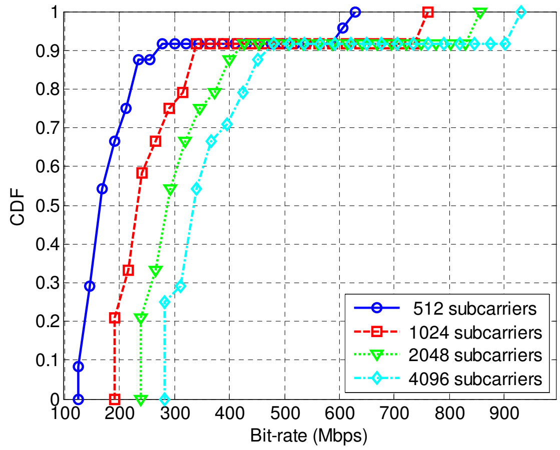


Fig. 8. CDF of the bit-rate for the off state as a function of the number of subcarriers using the cyclic prefix lengths shown in Table III

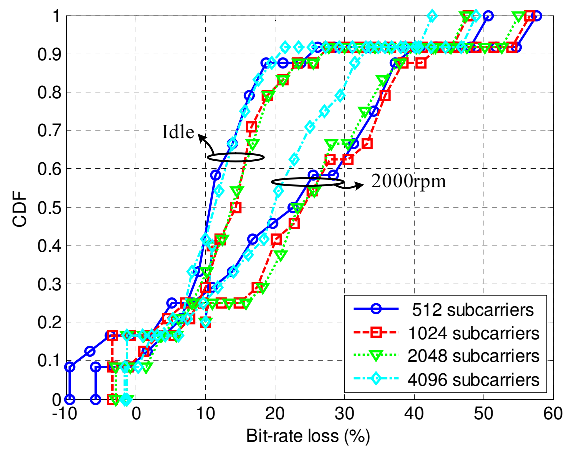


Fig. 9. CDF of the bit-rate loss for the idle and 2000 rpm states with respect to the achieved bit-rate for off state, as a function of the number of subcarriers using the cyclic prefix lengths shown in Table III

the achieved bit-rate in the off state for various number of subcarriers. Fig. 9 displays the influence of the engine state in the bit-rate. To this end, the CDF of the percentage bit-rate loss experienced in the idle and 2000 rpm states with respect to the bit-rate achieved in the off state have been computed. As seen, the largest bit-rate losses occur in the 2000 rpm state. In particular, losses are higher than 10% and 20% in 50% of the channels. However, the feasibility of PLC technology on in-vehicle channels is proved by the values presented in Fig. 8, where bit-rates higher than 160 Mbps for 512 subcarriers and higher than 330 Mbps for 4096 subcarriers are achieved in 50% of the analyzed channels.

## V. Conclusions

In this paper the suitability of using in-vehicle power lines as high-speed transmission medium has been assessed by evaluating the performance of an OFDM system. A set of representative measured channels and noise PSDs have been utilized to determine the parameters -number of subcarriers and cyclic prefix lengths- that maximize the performance. The influence of the engine state on the achievable bit-rate has been discussed and statistical results have been presented.

## Acknowledgment

This work has been supported by the Junta de Andalucía under proyect n$^o$ TIC-03007. The authors would like to thank to Fiat Málaga for their collaboration.

## References

[1] V. Degardin, M. Lienard, P. Degauque, and P. Laly, "Performances of the homeplug phy layer in the context of in-vehicle powerline communications," in *Power Line Communications and Its Applications, 2007. ISPLC '07. IEEE International Symposium on*, march 2007, pp. 93 –97.

[2] P. Tanguy, F. Nouvel, and P. Maziearo, "Power line communication standards for in-vehicule networks," in *Intelligent Transport Systems Telecommunications,(ITST),2009 9th International Conference on*, october 2009.

[3] M. Mohammadi, L. Lampe, M. Lok, S. Mirabbasi, M. Mirvakili, R. Rosales, and P. van Veen, "Measurement study and transmission for in-vehicle power line communication," in *Power Line Communications and Its Applications, 2009. ISPLC 2009. IEEE International Symposium on*, april 2009, pp. 73–78.

[4] A. B. Vallejo-Mora, J. J. Sánchez-Martínez, F. J. Cañete, J. A. Cortés, and L. Díez, "Characterization and evaluation of in-vehicle power line channels," in *Proceedings of the 53th Annual IEEE Global Telecommunications Conference (GLOBECOM)*, 2010.

[5] J. J. Sánchez-Martínez, A. B. Vallejo-Mora, J. A. Cortés, F. J. Cañete, and L. Díez, "Evaluación de las prestaciones de un sistema OFDM sobre la red de alimentación de un vehículo," in *XX Jornadas Telecom I+D*, September 2010.

[6] M. Lienard, M. O. Carrion, V. Degardin, and P. Degauque, "Modeling and analysis of in-vehicle power line communication channels," *IEEE Transactions on Vehicular Technology*, vol. 57, no. 2, pp. 670–679, March 2008.

[7] International Electrotechnical Commission (IEC), "CISPR 25: Radio disturbance characteristics for the protection of receivers used on board vehicles, boats, and on devices. Limits and methods of measurement," 2002-08.

[8] E. Lee and D. Messerschmitt, *Digital Communication*. Kluwer Academic Publishers, 1994.